

Article

Abrupt High PM Concentration in an Urban Calm Cavity Generated by Internal Gravity Waves and a Shallow Coastal Atmospheric Boundary Layer with the Influence of the Yellow Dust from China

Doo-Sun Choi ¹, Soo-Min Choi ² and Hyo Choi ^{1,*} 

¹ Atmospheric & Oceanic Disaster Research Institute, Dalim Apt. 209 ho, Songjungdong 940-23, Gangneung 25563, Republic of Korea

² Department of Computer Engineering, Konkuk University, 268 Chungwon-daero, Chungju 27478, Republic of Korea

* Correspondence: du8392@hanmail.net

Abstract: Using GRIMM-1107 aerosol sampler, GOES-9 DCD satellite images, HYSPLIT model of backward trajectory and 3D-meteorological WRF-3.6 model, high particulate matter concentrations were investigated at Gangneung city in the Korean east coast which consists of Mt. Taeglyung in its west and the East Sea in its east on 00:00LST March 26~00:00 LST 4 April 2004. During a Yellow Dust period, the maximum PM₁₀ (PM_{2.5} and PM₁) concentration at the city was about 3.3 (1.1 and 1.01) times higher than one in the non-dust period. After the transported dust from the Gobi Desert and Nei-Mongo by strong northwesterly wind passed over Mt. Taegulyang and moved down toward the city. Then the dust was trapped inside a calm cavity generated by the confront of internal gravity waves (IGW) over the city and the eastward movement of the trapped dust is prohibited by the easterly onshore wind from the East Sea, and the trapped dust further combined with particulate and gaseous emitted from the road vehicles and heating boilers of the city at 09:00LST, March 30 (beginning time of office hours), causing high PM concentrations. On mid-day, as the combined dust due to daytime sufficient thermal convection rises up to the top of the thermal internal boundary layer (TIBL) of a 300 m depth from the coast to the top of the mountain, the ground-based PM concentrations in the city are much lower at 15:00LST due to the higher thickness of the TIBL than at 09:00LST. At night, particulates emitted from many road vehicles after the end of office hours and residential heating boilers could combine with both dust transported from the Nei-Mongo and falling dust uplifted from the ground surface of the city during the day, and they were trapped inside a calm cavity by the IGW under much shallower stable nocturnal surface inversion layer than the TIBL, causing more dust to be accumulated near the surface and showing the maximum PM concentrations at 20:00 LST.



Citation: Choi, D.-S.; Choi, S.-M.; Choi, H. Abrupt High PM Concentration in an Urban Calm Cavity Generated by Internal Gravity Waves and a Shallow Coastal Atmospheric Boundary Layer with the Influence of the Yellow Dust from China. *Remote Sens.* **2023**, *15*, 372. <https://doi.org/10.3390/rs15020372>

Academic Editor: Jing Wei

Received: 13 November 2022

Revised: 28 December 2022

Accepted: 28 December 2022

Published: 7 January 2023

Keywords: PM₁₀; PM_{2.5}; PM₁; WRF-3.6 model; GOES-9 DCD satellite images; HYSPLIT model; Gobi Desert; internal gravity waves; thermal internal boundary layer; nocturnal surface inversion layer; potential vorticity



Copyright: © 2023 by the authors. Licensee MDPI, Basel, Switzerland. This article is an open access article distributed under the terms and conditions of the Creative Commons Attribution (CC BY) license (<https://creativecommons.org/licenses/by/4.0/>).

1. Introduction

Asian Dust with various names of Dust Storm, Sand Storm, Yellow Sand, or KOSA mainly originated from Taklamakan, Gobi, and Ordos deserts and Loess plateau in northern China under a relative humidity of air less than 40% and wind velocity for the dust mobilization over 10 m/s in the dry seasons of March, April and May (spring) and October (fall) [1–4]. Dust Storms can remove several hundred thousand tons of both sand and dust from the desert and dry areas in northern China [5–8].

50% of the total amount of dust [9–12] is deposited under the long-range transport process toward the downwind side countries such as Taiwan, Korea, Japan, and even

the western parts of Canada and the U.S.A., resulting in very low visibility and worse air quality [13–20]. Most previous research on the transported dust from northern China toward the Korean peninsula has been focused on the local loading and chemical composition analysis of dust, observation study of dust using lidar and satellite images, and synoptic-scale meteorological analysis on the dust transportation route [21–23].

Choi and Choi [24] insisted that a large number of dust particles transported from the Gobi Desert were trapped within the daytime convective boundary layer (CBL) in the mountain basin in the west of the city by the covering of the upper inversion layer (UIL) like a lid. It means that the trapped dust below the UIL was uplifted by the increase of the daytime thermal convection near the ground surface, a few hours later and could move over the mountain top. At night, the dust particles moved toward the downwind city along its lee side downslope and merged in the shrunken nocturnal inversion layer of the city, due to the decrease of ground-based air temperature. Choi et al. [25] proved that a sudden high concentration of total suspended particulate matter near the ground surface was detected below the shrunken CBL due to the intrusion of cold air by the passage of a cold front in the Seoul metropolitan area during the day for a dust storm period.

Choi et al. [26] showed that using a three-dimensional (3D) non-hydrostatic meteorological model with a terrain-following coordinate system (x, y, z^*) connected with a 3D random walk model of particles with a constant depth of terrain-following coordinate system ($x, y, z+$), the recirculation of suspended particulates by the interaction of sea-land breeze circulation and coastal atmospheric boundary layer in the complex terrain of the Korean east coast was displayed in detail. In a similar way, Choi and Speer [27] also presented the effects of atmospheric circulation and boundary layer structure on the dispersion of suspended particulates in the Seoul metropolitan area numerically, using a 3D random walk model of particles.

However, when an individual researcher operates two numerical models linked to each other, the preparation of direct measurement data of the real time emission amounts of air pollutants, or calculated data of pollutants by indirect methods using empirical equations in order to make input data for the model grid points is difficult, and it takes a lot of calculation time to get simulation results, resulting in a disadvantage of time and finance. In their research, the formation of sudden high concentrations of particulate matter for a few hours, related to the trapping of dust inside a calm cavity generated by internal gravity waves in the lee side of the mountain was not explained.

Holton [28]) explained that internal gravity waves are transverse waves in which the parcel oscillations are parallel to the phase lines, and a parcel displaced a distance along a line tilted at an angle to the vertical direction. Internal gravity waves are waves occurring in the interior of a stratified fluid, with buoyancy providing the restoring force which opposes vertical displacements. Such waves are ubiquitous in the atmosphere and ocean and are the internal counterpart to the familiar surface gravity waves. In general, internal gravity waves are generated by flow over topography, convective storms, and imbalance of large-scale circulations.

Choi et al. [26] explained numerically the recycling of suspended particulates by the interaction of sea-land breeze circulation and complex coastal terrain, considering internal gravity waves in the eastern mountainous coast of Korea. When a strong westerly wind blows over a high mountain and along the steep face of the eastern slope of the mountain, internal gravitational waves are created. The increase of wind speed causes the development of internal gravity waves on the lee side of the mountain and these waves produce a bounding up and down motion with a hydraulic jump up to a height of about 1 km above the surface over the city. Particulate matter driven by strong westerly wind near the top of the mountains also descends its eastern slope, reaching the city area in a coastal basin and merges near the surface, especially inside the nocturnal surface inversion layer.

The purpose of this study was to investigate the occurrence of abrupt high particulate matter concentrations inside a cavity generated by internal gravity waves along

the mountain slope and the variability of atmospheric boundary layer depth for day or night in a coastal city of Korea during a Yellow Dust period in spring. For this study, NOAA GOES-9 DCD (the U.S. National Oceanic and Atmospheric Administration's Geostationary Operational Environment Satellite System; dust color detection) satellite images and NOAA-HYSLPIT (the Hybrid Single-Particle Lagrangian Integrated Trajectory) backward air trajectory model were used for analyzing transportation routes of dust toward Gangneung city of Korea. A 3D meteorological model—WRF v. 3.6.1 (Weather Research & Forecasting model) for generating synoptic scale, mesoscale, and microscale wind fields, atmospheric boundary layer, and trapping of air masses near the ground surface in the coast and over the open sea surface by calculating potential vorticity as a tracer of air particles in detail.

2. Topographical Feature and Measurement of Particulate Matters

2.1. Topography of Study Area

The study area includes Gangneung city ($37^{\circ}45'N$, $128^{\circ}54'E$; a basin of 20 m over mean sea level) in the Korean eastern mountainous coast, which consists of high mountains in the west of the city, and the East Sea (/ the Japan Sea) in the east in Figure 1. GRIMM aerosol sampler-1107 (German product; approved by The Ministry of Environment, Korean Government) was established to gather hourly particulate matter- PM_{10} , $PM_{2.5}$, and PM_1 concentrations at Gangwon Regional Meteorological Administration in the central part of Gangneung city adjacent to the East Sea. The dust originated from the Gobi Desert (southern Mongolia; G) and Nei-Mongo area (northern China) passed through the Korean peninsula and reached Gangneung city.

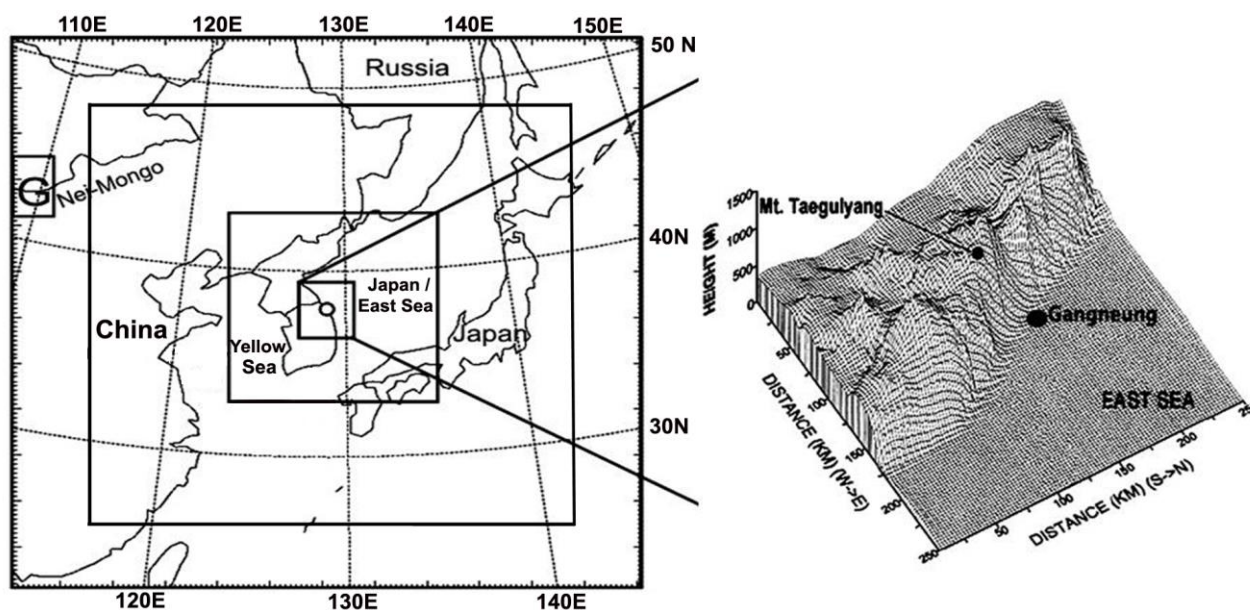


Figure 1. Topographical features in the vicinity of the Korean peninsula (left) including Gangneung city (right), in which an aerosol sampler was equipped [24,29,30]. Big and small squares inside the left figure denote the first, second, and third domains with sequential horizontal grid spaces of 27 km, 9 km, and 3 km covering a 91×91 grid number for numerical simulation using WRF-3.6 model. G (a small square in the left) denotes the Gobi Desert.

2.2. Measurement of Particulate Matters

The aerosol sampler of GRIMM Model-1107 is a monitoring system measures particulates via laser-light scattering and was equipped at Gangwon Meteorological Administration in the downtown area of Gangneung city from March 26 to 4 April 2004, in spring. Air containing multiple particle sizes passes through a flat laser beam produced by a precisely focused laser and several collimator lenses. The scattered light is then detected

by a 15-channel, pulse-height analyzer for size classification to measure 15 sizes of dust particles ($>0.3 \mu\text{m}$ to $20.0 \mu\text{m}$), which can measure the concentration of particulate matter ($\mu\text{g}/\text{m}^3$) at a 5-min interval.

Then, the concentrations are again summed into PM_{10} (the total amount of a particle size of $10 \mu\text{m}$ or less), $\text{PM}_{2.5}$ (with the total amount of $2.5 \mu\text{m}$ size or less), and PM_1 (with the total amounts of $1 \mu\text{m}$ size or less). For our research, the concentrations of PM_{10} , $\text{PM}_{2.5}$, and PM_1 are recalculated as the 1 h-averaged value and these concentrations were used as the basic data for this study.

3. Numerical Method and Input Data

A three-dimensional Weather Research & Forecasting Model (WRF)-3.6.1 (<https://www.mmm.ucar.edu/models/wrf> accessed on 20 September 2019) was adopted for a 96-h numerical simulation on meteorological elements such as wind, temperature, potential temperature, potential vorticity, etc., in northeastern Asia including Gangneung city in the Korean east coast from 00:00 UTC (Local Standard Time (LST) = 9 h + UTC), March 29 through 00:00 UTC, April 2, 2004. In the numerical simulation, one way, triple nesting process from the first domain to the third domain was performed with horizontal grid spaces of 27 km, and 3 km covering a 91×91 grid number in each domain, respectively

National Center for Environmental Prediction/National Center for Atmospheric Research (NCEP/NCAR) reanalysis-Final Analyses (FNL) 1.00×1.00 resolution data (<https://rda.ucar.edu/datasets/ds083.2/> accessed on 20 September 2019) were used as meteorological input data to the model and vertically interpolated onto 36 levels with sequentially larger intervals increasing with a height from the surface to the upper boundary level of 100 hPa. In the model, WSM 6 scheme was used for heat and moist budgets and microphysical processes in the atmospheric boundary layer and the YSU PBL scheme was adopted for the planetary boundary layer.

The Kain-Fritsch scheme (new Eta) was adopted for cumulus parameterization and the fifth thermal diffusion model was for the land surface. Simultaneously, the RRTM longwave radiation scheme and the Dudhia short-wave radiation schemes were also used. Meteorological elements evaluated by the model are verified by hourly archived wind, air temperature, and relative humidity measured by Gangwon Regional Meteorological Administration in Gangneung city.

4. Results

4.1. Before a Dust Period

4.1.1. Dust Transportation and Particulate Matter Concentration (PM)

Hourly concentrations of PM_1 , $\text{PM}_{2.5}$, and PM_{10} were investigated at a Korean eastern coastal city, Gangneung from 00:00 LST March 26 to 00:00 LST 4 April 2004. This city has no industrial facilities, and the density of pine trees in the city is very high. The main air pollution source is only confined to vehicles on the road and heating boilers from the residential area. For a non-dust period before the influence of dust transported from the Gobi Desert and Nei-Mongo in northern China to a Korean eastern coast until 07:00 LST, March 29.

PM_{10} , $\text{PM}_{2.5}$ and PM_1 concentrations at the city were very low and their maximum (minimum) values of each particulate matter concentrations were $72.33 \mu\text{g}/\text{m}^3$ ($12.53 \mu\text{g}/\text{m}^3$), $41.00 \mu\text{g}/\text{m}^3$ ($6.75 \mu\text{g}/\text{m}^3$) and $35.33 \mu\text{g}/\text{m}^3$ ($5.82 \mu\text{g}/\text{m}^3$), respectively (Figure 2). Thus, very high PM_{10} concentrations for a dust period should be greatly affected by coarse particulate matter with diameters greater than $2.5 \mu\text{m}$, because $\text{PM}_{2.5}$ and PM_1 concentrations did not much changed regardless before or during the period of dust.

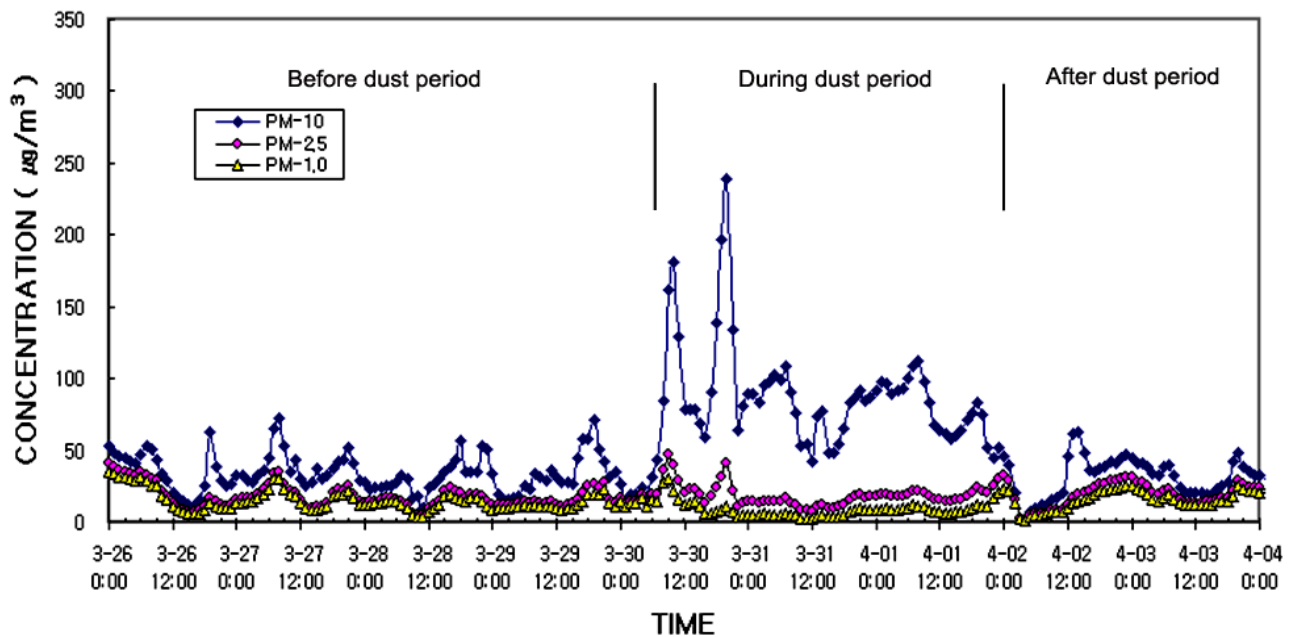


Figure 2. Hourly concentration ($\mu\text{g}/\text{m}^3$) of PM_{10} , $\text{PM}_{2.5}$, and PM_1 at an aerosol sampling point of Gangwon Meteorological Administration ($37^\circ 45' \text{N}$, $128^\circ 54' \text{E}$; 20 m height over the Mean Sea Level) in Gangneung city, from March 26 to 4 April 2004.

Figure 3a showed that GOES-9 DCD satellite picture reflects the dust particle dispersion and density with the distribution of dust (green color (light) to bole color (dense)) originating from the Gobi Desert (square) and Nei-Mongo on the left of a cold front to move to Manchuria, China near the northern border of Korea at 09:00 LST, March 29. (https://en.wikipedia.org/wiki/Geostationary_Operational_Environmental_Satellite accessed on 31 March 2004)

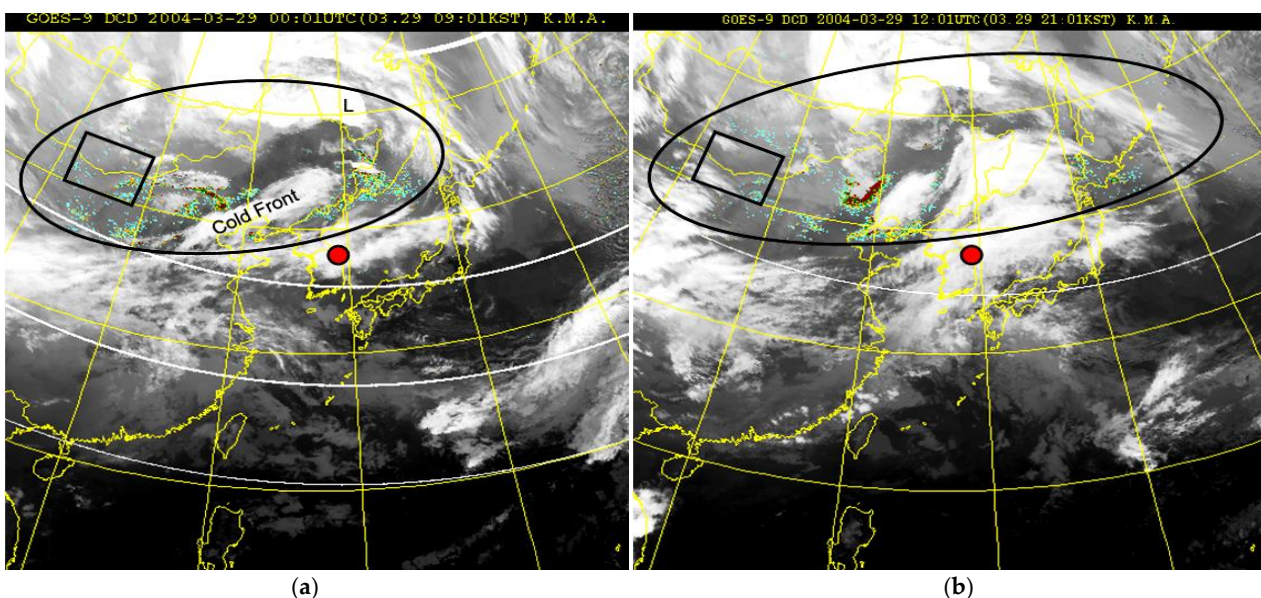


Figure 3. GOES-9-DCD satellite picture at (a) 09:01 LST, 29 March 2004, and (b) 21:01 LST. The blue color area denotes the dust originating from the Gobi Desert (a small square) on the left of Cold Front to move toward Nei-Mongo in the east of the desert and southern Manchuria near the border of northern Korea. The large circle and small one denote the area of dust dispersion and Gangneung city of Korea, respectively.

From the surface weather map at 09:00 LST, one can expect that a dust storm could be generated in the Gobi Desert behind the cold front (left-hand side) in Figure 3a, and Figure 4a, where strong northerly surface wind prevailed, passing by the Gobi Desert and Nei-Mongo area. Then the dust were uplifted and dispersed eastward to Manchuria in northeastern China and northern Korea by the southwesterly wind in Figure 3a.

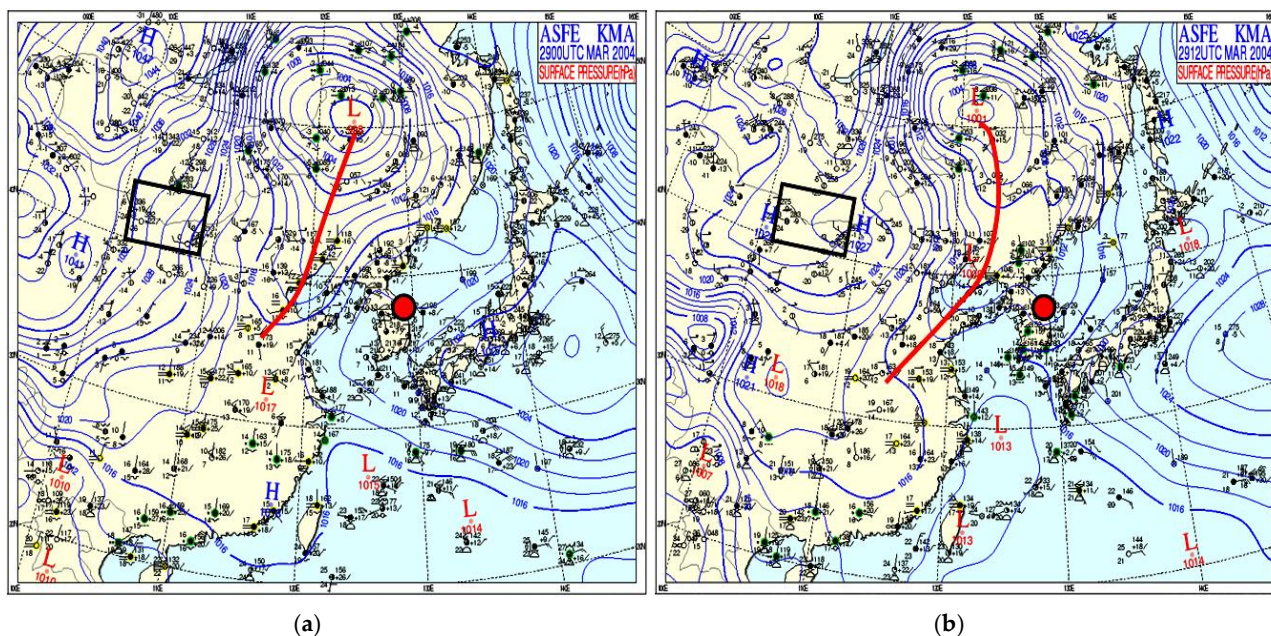


Figure 4. Surface pressure and at (a) 09:00 UTC (00:00 LST), 29 March 2004, and (b) 12:00 UTC (21:00 LST). A small square, a thick red line, and a small circle denote the Gobi Desert, the cold front, and Gangneung city, respectively.

As time went on, the cold front moved eastward and the dust driven by the wind also moved eastward and southeastward. At 21:00 LST, March 29, the area of dust dispersion under the similar wind pattern extended more widely, especially reaching Shalalin in southern Russia (upper right of the figure) and Hokkaido in northern Japan, but not reaching Gangneung city on the Korean east coast, respectively, resulting in no influence on the increasing of PM at the city (Figures 2, 3b and 4b).

The NOAA HYSPLIT model is a complete system for computing simple air parcel trajectories, as well as complex transport, dispersion, chemical transformation, and deposition simulations. HYSPLIT continues to be one of the most extensively used atmospheric transport and dispersion models in the atmospheric sciences community. A common application is a back trajectory analysis to determine the origin of air masses and establish source-receptor relationships. This model has also been used in a variety of simulations describing the atmospheric transport, dispersion, and deposition of pollutants and hazardous materials. (<https://www.arl.noaa.gov/hysplit>) (accessed on 22 December 2020).

In order to understand whether the dust transported from the Gobi Desert and Nei-Mongo caused the increase of particulate matter concentrations at Gangneung city, the NOAA HYSPLIT model of backward trajectories of air particles was used, setting up the height of air particle trajectory as 2000 m, 1000 m and 500 m at Gangneung city, respectively (Figure 5a,b). Dust particles originating from 6000 m height of Moscow, Russia on March 25, passed by about 3000 m height of the Gobi Desert and Nei-Mongo on March 27-Bohai Sea and Yellow Sea on March 28, and finally reached 2000 m height of Gangneung city at 00:00 UTC (09:00 LST), March 29. Eventually, these dust particles passing by 3000 m height of the Gobi Desert could not affect the ground-based particulate matter concentration of Gangneung city.

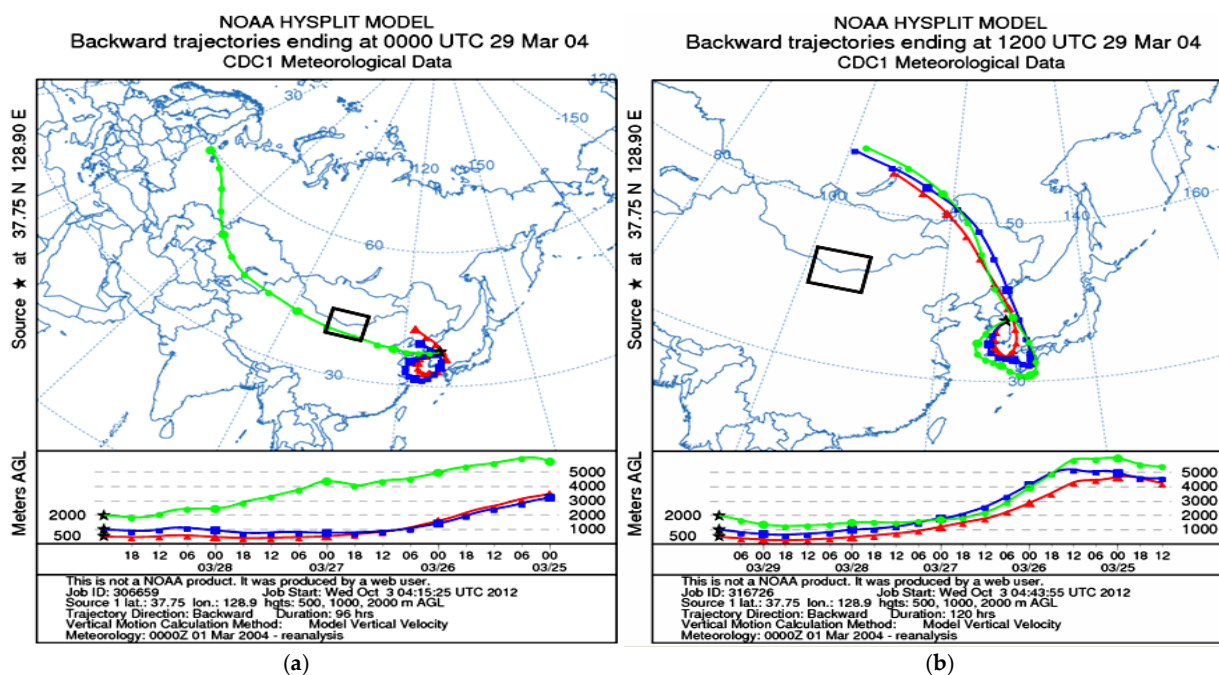


Figure 5. Backward trajectories of air masses by NOAA HYSPLIT model for 4 days were at 2000 m, 1000 m, and 500 m heights of Gangneung city, ending at (a) 00:00 UTC (09:00 LST), 29 March 2004, and (b) 12:00 UTC (21:00 LST). Air particles reaching 500 m, 1000 m, and 2000 m heights of Gangneung city should not influence the increases of ground-based PM of the city, even though air trajectory over 5000 m height passed through the Gobi Desert and finally reached 2000 m height of Gangneung city, which was too high to be away from the ground surface.

Thus, even though air particles passed by the Gobi Desert and Nei-Mongo at about 3000 m height, air particles arrived at 2000 m height of Gangneung city can not affect the ground-based PM concentrations. At the same time, air particles arrived at 500 m and 1000 m height of Gangneung city came from the southern Yellow Sea and Kyushu Island (clean air masses), and thus, these particles did not come from the Gobi Desert or Ne-Mongo to Gangneung city (Figures 3a and 5a).

However, all particles departing from 6000 m~4000 m heights near the Baikal lake on March 25 passed by Jilin Province of the north-eastern China-Manchuria-the Korean eastern coast-the South Sea of Korea-its western coast, and flew below 2000 m height through the surface on March 28 and 29. Finally, they finally reached the city at 21:00 LST, March 29 (Figures 3b–5b). These particles passing this route did not include a great amount of dust floated from the desert or Nei-Mongo and reached Gangneung city. Thus, as the dust originating from the Desert did not reach Gangneung city, maximum concentrations of PM_{10} , $PM_{2.5}$, and PM_1 were attributed to only the dust and gaseous emitted from the city on the coast.

4.1.2. Effects of Wind and Atmospheric Boundary Layer on High PM Concentrations

Before the intrusion of yellow dust from the Gobi Desert and Nei-Mongo toward the city, an increasing (decreasing) trend of PM_{10} concentration was apparent, as both $PM_{2.5}$ and PM_1 concentrations increased (decreased), and this concentration was affected by only local air pollutants. High PM_{10} , $PM_{2.5}$, and PM_1 concentrations near the surface of the city were detected from 07:00 LST~09:00 LST around the beginning of office hour, by pollutants emitted from vehicles on the road with a high traffic density.

Southwesterly wind in the basin of Mt. Taegualung (here, T) in the west of Gangneung city at 09:00 LST, March 29 flew over the top of the mountain toward the coastal city and intensified into a strong downslope wind of 6 m/s~13 m/s along the eastern slope of the mountain to be bounded up and down over the Gangneung coast, depicting westerly internal gravity waves (IGW) in Figure 6a,b, and Figure 7a. Thus, particulate matter and

gaseous emitted from the ground surface of the city easily merged inside a small calm cavity over the city below the IGW, causing a high PM₁₀.

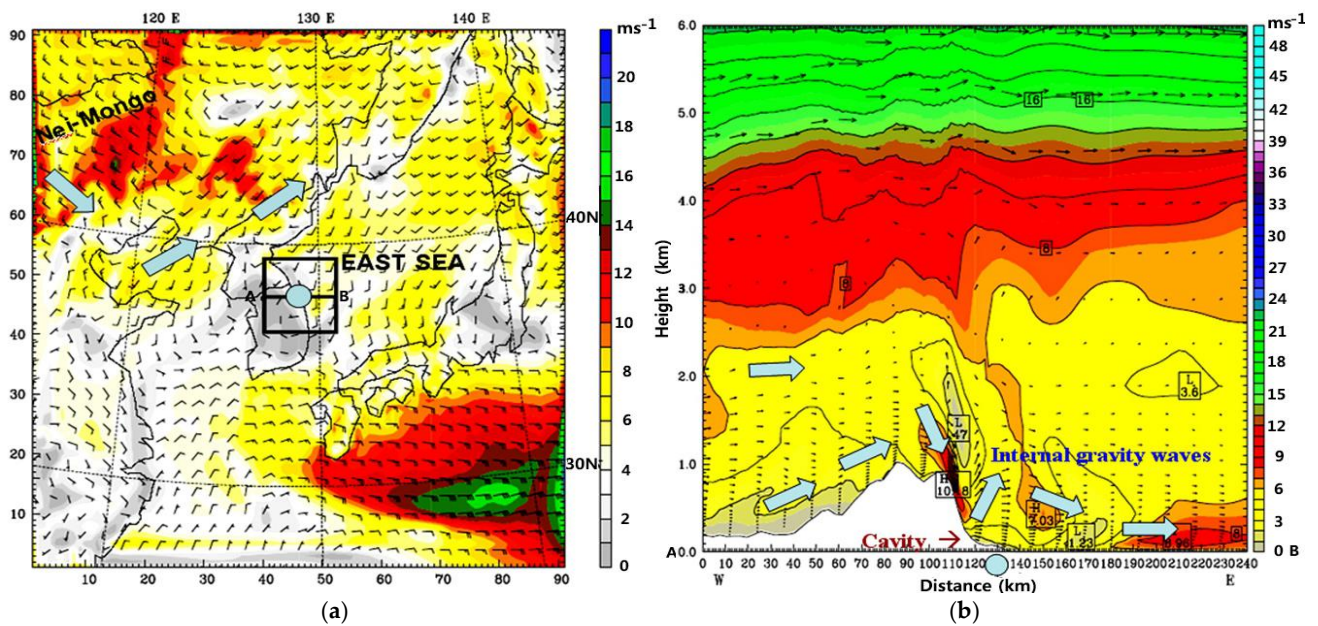


Figure 6. (a) Surface wind (m/s) in north-eastern Asia (the first domain of a horizontal grid interval of 27 km) including the vicinity of Gangneung city on the Korean east coast (a small square; the third domain of 3 km grid interval in the WRF model simulation) at 09:00 LST, 29 March 2004, and (b) vertical profile of horizontal wind (m/s) on a straight cutting line in A-B (a). A small circle denotes Gangneung city. Southwesterly strong downslope wind could generate an IGW bounding up and down in the vicinity of the city in (b). The dusts emitted from the city merged below the IGW, causing a high PM₁₀ concentration in Figure 2.

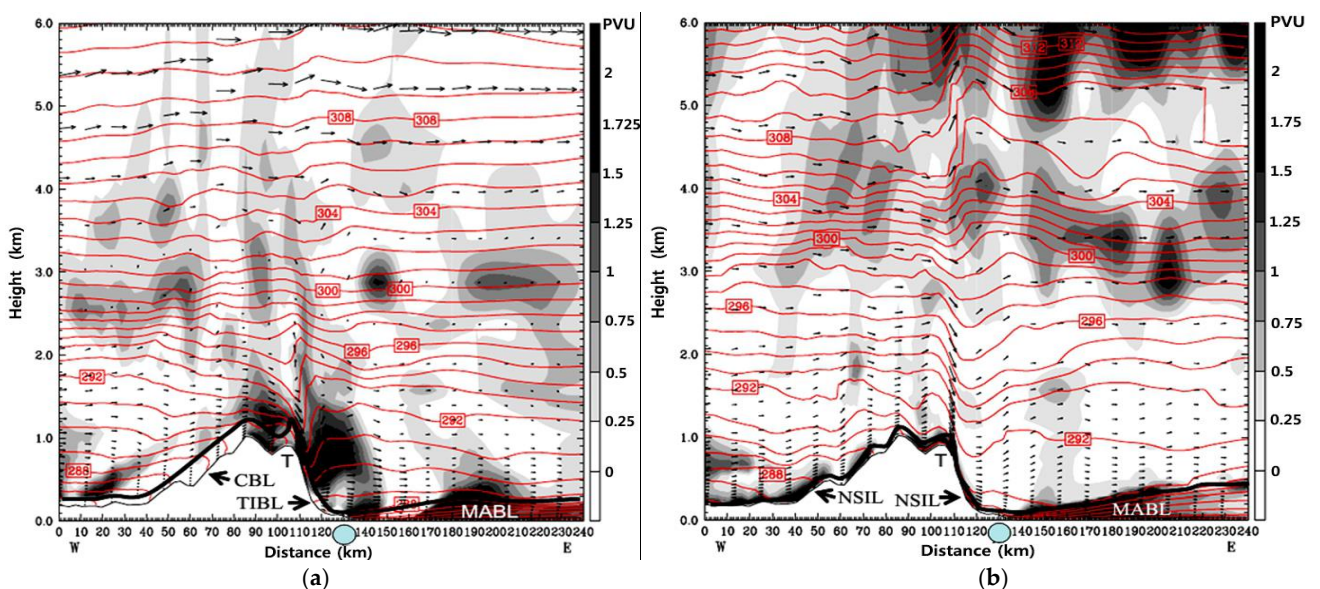


Figure 7. Vertical profile of potential temperature (k) and wind speed (m/s) in the third domain of WRF-3.6 model simulation at (a) 09:00 LST, 29 March 2004, and (b) 21:00 LST. Thick line, CBL, TIBL, MAIL, NSIL, T, and a small circle on the bottom in (a,b) denote the top of the convective boundary layer, convective boundary layer, thermal internal boundary layer, marine atmospheric boundary layer, nocturnal surface inversion layer, Mt. Taegulyang, Gangneung city, respectively. The dark area of high potential vorticity near the surface in the coastal and open seas denotes trapped air particles, which are well matched with high PM concentrations [29].

Rossby [31,32] found that potential vorticity (PV) on isentropic surfaces was conserved for frictionless and adiabatic flow. PV is defined by the variation of potential temperature to atmospheric pressure with height ($\frac{\partial\theta}{\partial p}$). Reed and Sanders [32] used PV as a tracer of air particles in middle-and upper tropospheric fronts originating in the stratosphere. Reed and Sanders [33], Sanders and Gyakum [34], Reed and Albright [35], and Chen et al. [36] explained cyclogenesis and the development of a frontal zone using the vorticity theory. Haynes and McIntyre [37] indicated that Ertel's potential vorticity (Ertel's PV; baroclinic potential vorticity) with diabatic heating and frictional terms could be diluted or concentrated only by the flow across isentropic surfaces in the isentropic coordinate (x, y, θ). If diabatic heating or frictional torques are present, PV is no longer conserved, and PV can be created or destroyed, resultantly being drawn away from the isentropes.

Although Ertel's potential vorticity theory has usually been focussed on the relatively large-scale motion of air, this theory can be adapted to chase the tracer of air particles in the atmospheric boundary layer with a comparatively much smaller scale of meteorological phenomena. Adopting this theory, Choi and Zhang [4] predicted duststorm evolution with Ertel's potential vorticity in the Gobi Desert of southern Mongolia and Choi et al. [38] also elucidate the transport and accumulation of yellow dust in the coastal atmospheric boundary layer with denser PV values. It means that the area of the high PM concentrations is well matched with the area of dense potential vorticity. In our research, using Ertel's potential vorticity theory to chase the merging area of particulate matters, the dark shadow area presenting high potential vorticity in Figure 7a,b was detected near the surface of the coast and open sea, denoting the trapped air particles and showing well matched high PM concentrations in Figure 2.

Around 09:00 LST (beginning of office hour) on a sunny day, a convective boundary layer (CBL) of about 300 m in the western inland basin of Mt. Taegulyang and a thermal internal boundary layer (TIBL) of about 150 m in the coastal basin toward the top of the mountain can be generated by the thermal convection of air due to the thermal heating of the ground surface by solar radiation (Figures 6b and 7a), but they are relatively shallow due to insufficient thermal convection than ones at 15:00 LST (Figure 8a,b). Thus, a significant amount of particulate matter and gaseous emitted from both vehicles on the road and heating boilers in the residential area of the city on the relatively cool weather in the morning merged inside a shallow TIBL (Figure 7a), resulting in high PM concentrations around this time (Figures 2 and 6b).

In Figure 8a,b, the CBL at 15:00 LST, March 29 on a mid-day is much developed vertically with a depth of about 1200 m in the western inland basin of Mt. Taegualung, under the sufficient thermal convection of air than 09:00 LST. At the same time, similar to the CBL, the TIBL in the coastal basin is also developed from the coast to the top of Mt. Taegulyang with a maximum depth of about 300 m, which is much shallower than the CBL [26]. The CBL and TIBL have the same generation mechanism, but the reason why the coastal TIBL is shallower than the inland CBL is to prohibit the vertical extension of the TIBL by the intrusion of relatively cool air from the cold sea toward the inland basin, resulting in the shrunken coastal CBL (that is, TIBL).

From 12:00 LST~15:00 LST, the moderate downslope wind could still produce internal gravity waves bounding up and down and a cavity over the Gangneung coast, in Figure 8a. Previously, Choi et al. [26] explained the recycling of suspended particulates by the sea-land breeze circulation and complex coastal terrain, using the 3D-meteorological model (MM5) connected with the Lagrangian particle model.

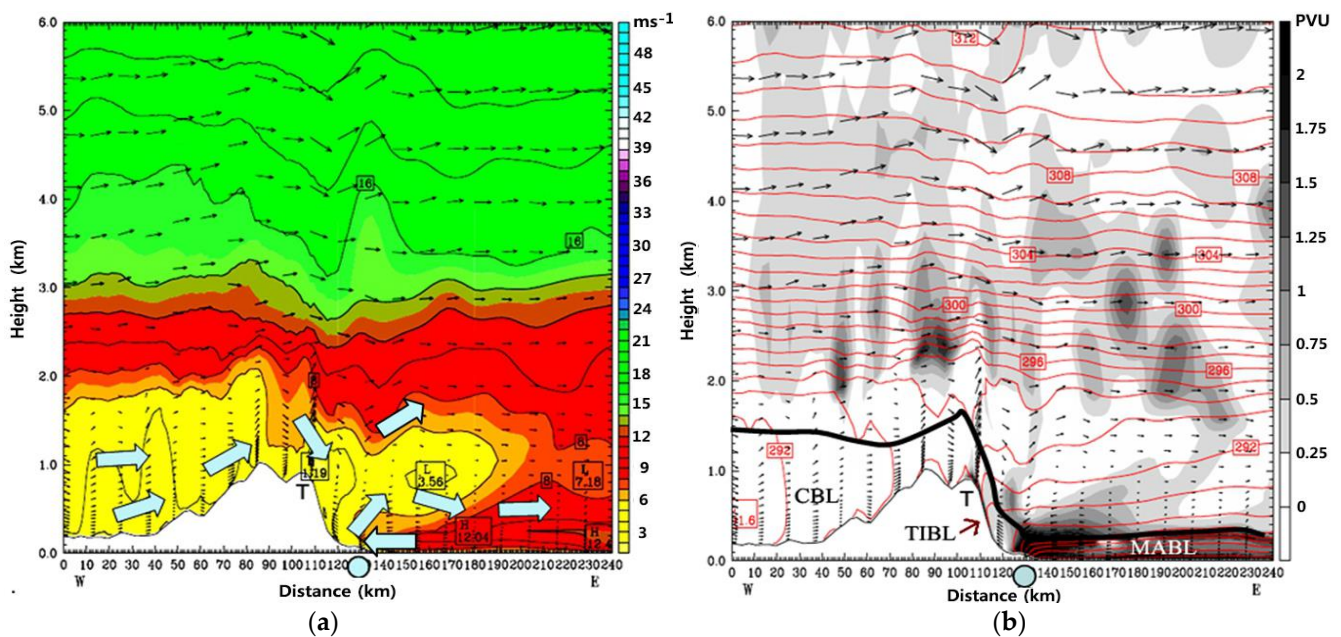


Figure 8. Vertical profile of (a) horizontal wind (m/s) and (b) potential temperature (k) with wind speed (m/s) in the third domain at 15:00 LST, 29 March 2004. The arrow, a small circle, the thick line, CBL, TIBL, and MABL denote wind, Gangneung city, the top of the convective boundary layer, convective boundary layer, thermal internal boundary layer, and marine atmospheric boundary layer. A dark area of high potential vorticity near the coastal and open sea surfaces denotes trapped air particles, showing high PM concentrations, but the uplifting of particulates in the TIBL toward a big cavity over the city in (a) causes a PM concentration near the city surface.

In general, as daytime goes on, strong thermal convection by the daytime heating of the ground surface can uplift air parcels including locally emitted particulate matters and gaseous to the top of the CBL in the inland basin or the TIBL in the coastal basin of our case, resulting in very low PMs near the surface around 12:00 LST~15:00 LST, but very high PMs at the top of the TIBL. Thus, as particulate matter emitted from the ground of the city should go up to the top of the TIBL and flow into the cavity over the coast near Gangneung city and then, the PM at the city ground must decrease in Figures 2 and 8a.

At 21:00 LST, March 29, southwesterly moderate wind prevailed in the vicinity of Gangneung city (Figure 9a). From the vertical profiles of horizontal wind, relatively strong downslope wind over 10 m/s generated internal gravity waves on the lee side of the mountain, and a smaller calm cavity than one at 09:00 LST existed over Gangneung city. At especially 21:00 LST, as the ground surface cooled due to no solar radiation causes the cooling of air masses near the surface, which can produce a stable lower atmosphere like shallow nocturnal surface inversion layer (NSIL) (Figure 7b). The NSIL in Figure 7b is much shrunken than the daytime CBL or the TIBL in Figure 8b.

The stable atmospheric condition can induce the falling of daytime floating particles to the top of the thermal internal boundary layer toward the ground surface. After sunset (that is, after the end of office hours) from 18:00 LST to 21:00 LST, the daytime uplifted pollutants fell down and combined particulate matter and gases emitted from the vehicles on the local road and heating boilers from the residential area. Then they could merge into the ground surface in a stable nocturnal surface inversion layer to be much shrunken than the daytime TIBL, resulting in maximum PM concentrations as shown in Figure 2. Our research shows a similar result to the previous work by Choi et al. [26].

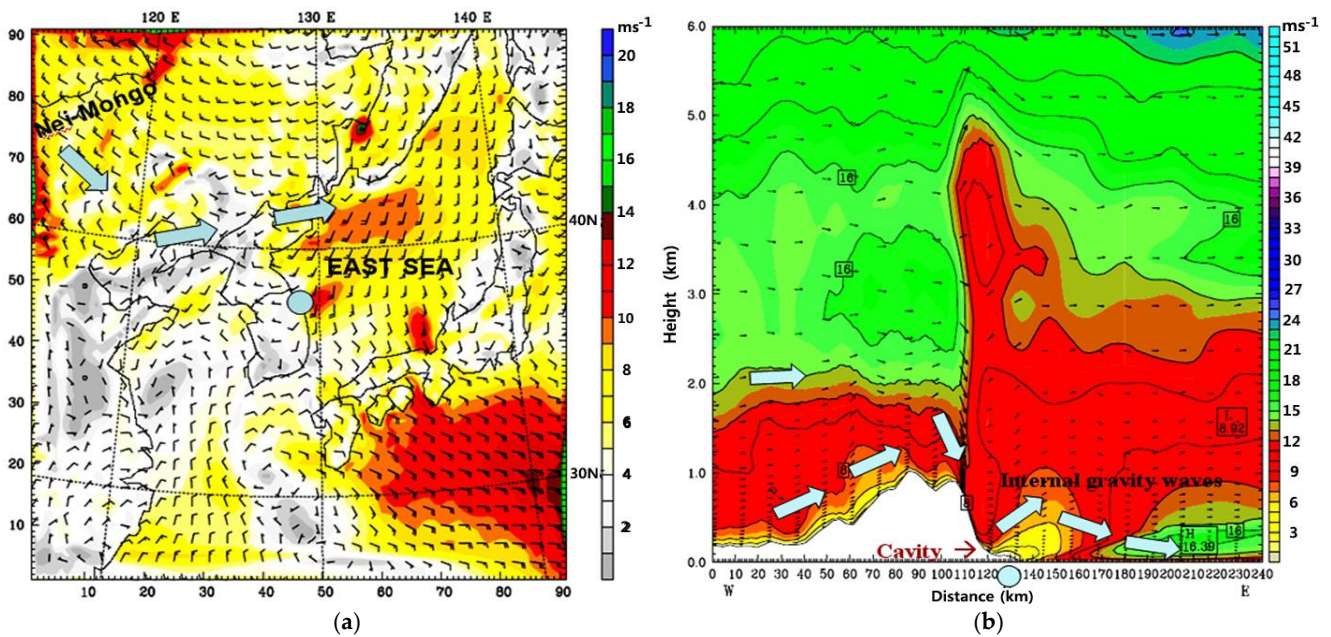


Figure 9. As shown in Figure 6, except for 21:00 LST, 29 March 2004. Southwesterly moderate wind prevailed in the vicinity of Gangneung city in (a) and dust emitted from the ground surface of the city merged inside a smaller calm cavity (city) below relatively moderate internal gravity waves in (b), resulting in a maximum PM_{10} concentration.

4.2. During a Dust Period

4.2.1. Dust Transportation and Particulate Matter Concentrations

During the dust period from 08:00 LST, March 30–00:00 LST, April 2, under the intensive intrusion of yellow dust from the Gobi Desert toward the city, maximum PM_{10} ($\text{PM}_{2.5}$ and PM_1) concentration was 3.3 (1.1 and 1.01) times higher than one of the non-dust period. Especially, when a large number of dust from Nei-Mongoo in northeastern China passed over Gangneung city on the Korean eastern coast, PM_{10} , $\text{PM}_{2.5}$, and PM_1 concentrations in the city reached $238.87 \mu\text{g}/\text{m}^3$, $46.50 \mu\text{g}/\text{m}^3$, and $30.25 \mu\text{g}/\text{m}^3$ at 20:00 LST, March 30.

On the other hand, their minima were $41.68 \mu\text{g}/\text{m}^3$, $7.17 \mu\text{g}/\text{m}^3$, and $2.77 \mu\text{g}/\text{m}^3$, indicating their maxima being at least five times larger than their minima (Figure 2). The maximum value of PM_{10} concentration for the dust period was three times larger than one before the dust period, but maximum $\text{PM}_{2.5}$ and PM_1 concentrations were similar to ones before the dust period. It means that very high PM_{10} concentrations for a dust period should be greatly affected by coarse particulate matters with their diameters greater than $2.5 \mu\text{m}$, because $\text{PM}_{2.5}$ and PM_1 concentrations did not much changed regardless before or during the period of dust.

Thus, coarse particulate matter larger than $2.5 \mu\text{m}$ of particle diameter made a major contribution to the increase of PM_{10} concentration during the dust period. GOES-9 DCD satellite pictures at 09:00 LST and 21:00 LST, on March 30 show that the dust originated from the Gobi Desert (a small square) and dispersed toward Nei-Mongoo in northeastern China, the Korean peninsula including Gangneung city (a small circle), Japan and the northern part of the Pacific Ocean and further the mid-China in the south (Figure 10a,b).

From the surface weather map at 09:00 LST, March 30 (Figure 11a), a cold front just passed by Gangneung city, and the wind pattern was changed from moderate southwesterly wind to strong northwesterly wind, which could easily induce the transportation of dusts from Nei-Mongoo in the northeastern China. At 21:00 LST, March 30, a great amount of dusts in Nei-Mongoo could pass by the city under strong northwesterly wind, resulting in maximum PM concentrations at 20:00 LST (Figures 2 and 11b).

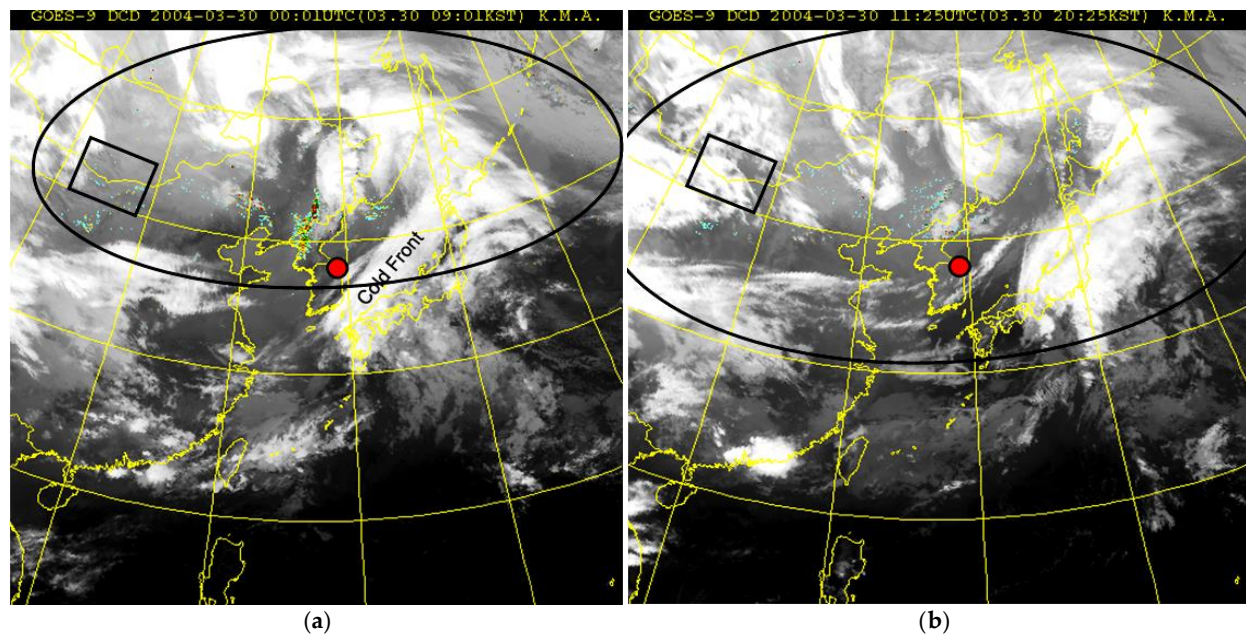


Figure 10. (a) GOES-9-DCD satellite picture at 09:01 LST, 30 March 2004, and (b) 20:25 LST. The blue color area denotes the dust originated from the Gobi Desert (a small square) and Nei-Mongo to disperse to Gangneung city (a small circle) on the Korean east coast in (a) and further dispersed toward the mid-China, Korean peninsula, Japan and the north-eastern Pacific Ocean.

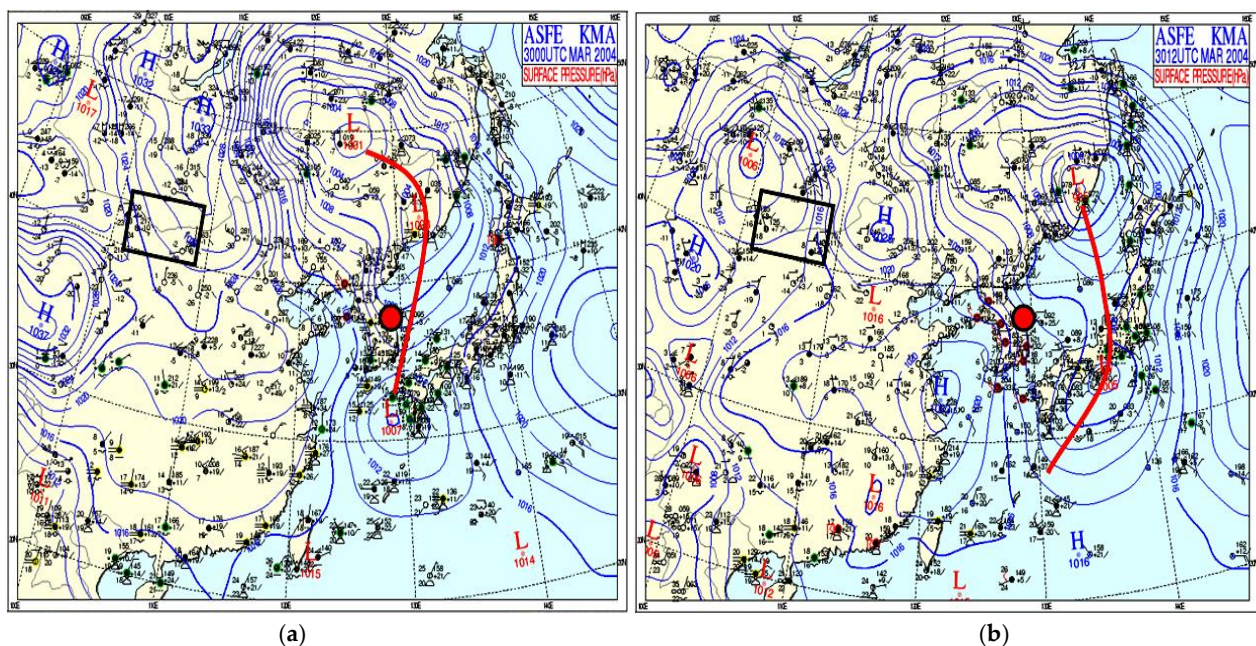


Figure 11. (a) Surface pressure at 09:00 UTC (00:00 LST), 30 March 2004, and (b) 12:00 UTC (21:00 LST). A small box, a thick red line, and a circle in (a) denote the Gobi Desert, cold front, and Gangneung city, respectively.

In Figure 12a, dust particles on the green color line originated from 6000 m height of southwestern Russia on March 27 passed by about 6000 m height of the Gobi Desert and Nei-Mongo on March 28, and the Bohai Sea and Yellow Sea on March 29 and finally reached at 3000 m height of Gangneung city at 09:00 LST (00:00 UTC), March 30. Thus, these particles did not include the dust in the lower atmosphere of the Gobi Desert and Nei-Mongo and can not affect the increase of the ground-based PM concentrations.

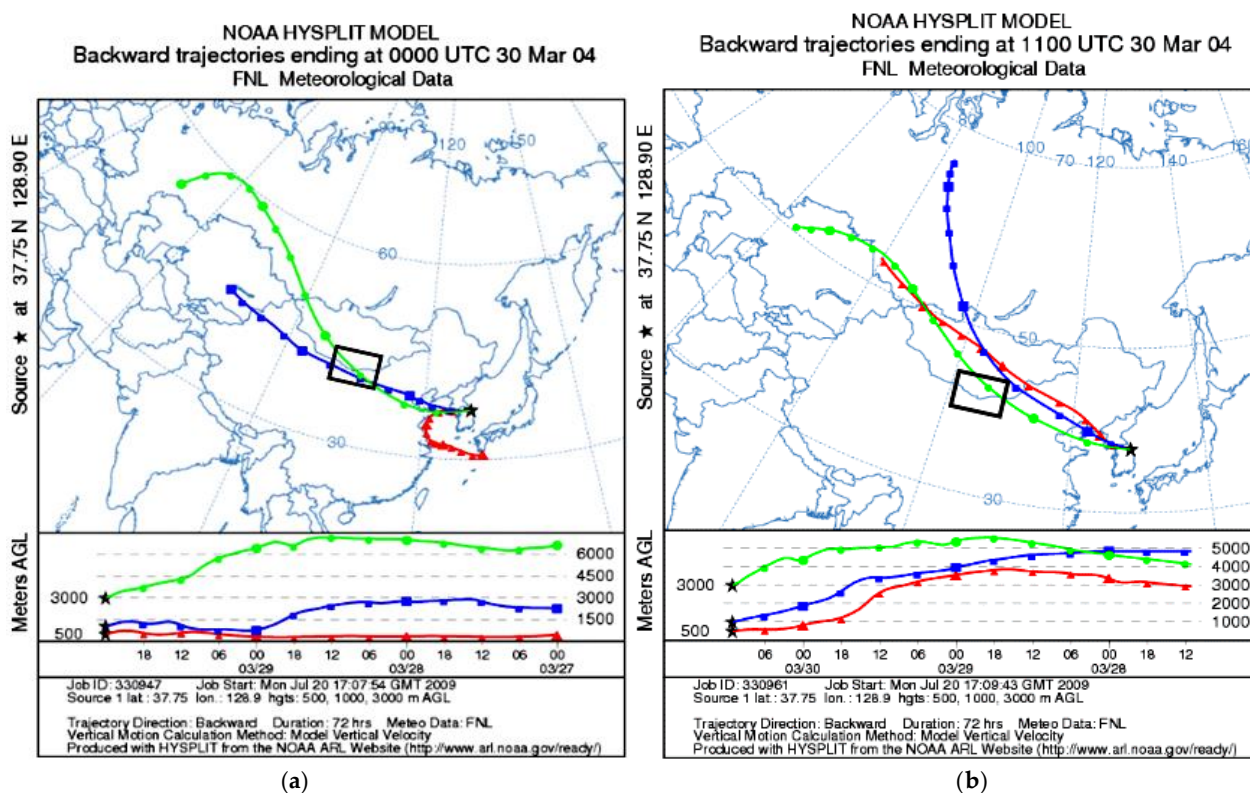


Figure 12. (a) Particle backward trajectory by HYSPLIT model at 09:00 UTC (00:00 LST), 30 March 2004, and (b) 12:00 UTC (21:00 LST)). A small square denotes the Gobi Desert.

Differently, as air particles on the blue line arrived at 500 m height of Gangneung city at 09:00 LST March 30 had originated from Kazastan passing by the Gobi Desert and Ne-Mongolia at the lower atmosphere from 3000 m toward 500 m, they could combine with dust particles raised from the Gobi Desert and Nei-Mongolia before 09:00 LST, March 29. Thus, they could give a great contribution to the increase of PM concentrations in Gangneung city.

However, as air particles on the red line at 100 m height of Gangneung city at 09:00 LST March 30 originated from the southern sea of Kyusu Island and passed by the Yellow Sea to reach Gangneung city, these particles did not give any contribution to the PM concentration of the city. In Figure 12b, at 21:00 LST, March 30, air particles started from the west of Mongolia at 3000 m~5000 m passed by both the Gobi Desert and Nei-Mongolia in the east of the desert and reached 3000 m~500 m of Gangneung city, resulting in the increase of PM concentrations, especially, showing a maximum PM₁₀ concentration at 20:00 LST, March 30.

Thus, as shown in Figure 13a,b, northwesterly wind induced a great number of dust from Nei-Mongolia into Gangneung city, where the dusts from Nei-Mongolia combined with particulate matter and gaseous emitted from the city and were trapped by opposite easterly wind from the East Sea of Korea, resulting in a very high PM concentrations at 09:00 LST.

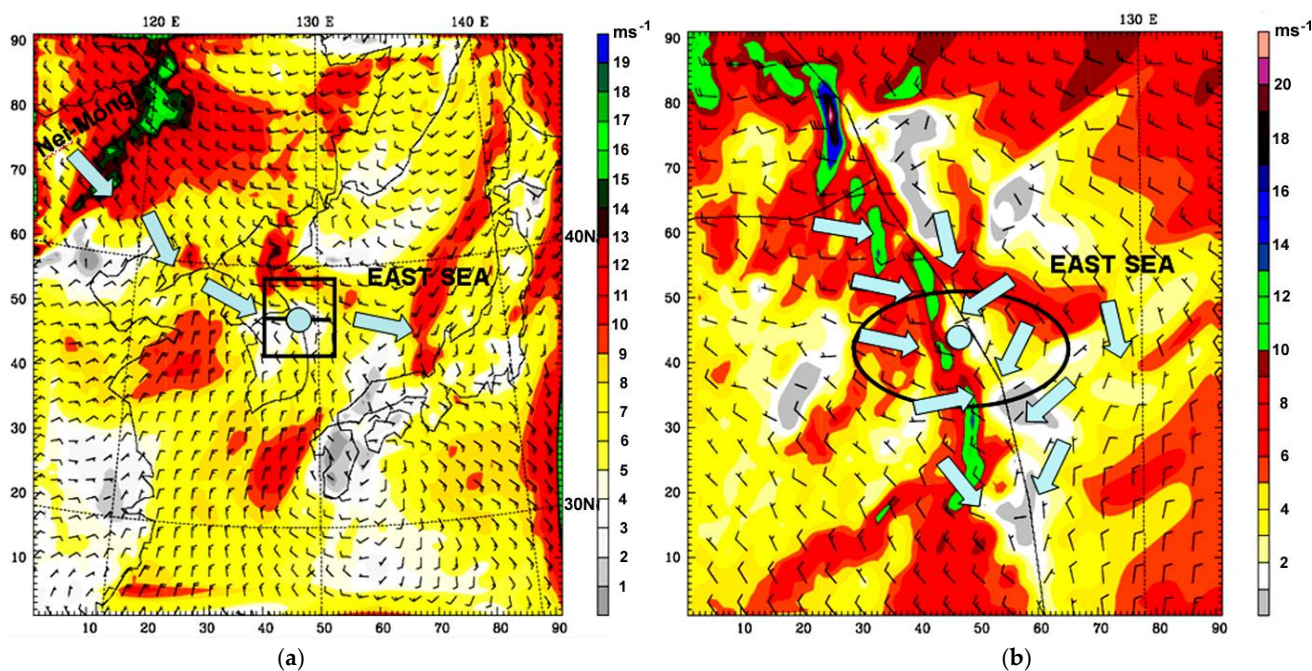


Figure 13. Surface wind (m/s) in (a) north-eastern Asia including Gangneung city on the Korean east coast (a small square; the first domain of WRF-3.6.1 model simulation) at 09:00 LST, 30 March 2004 and (b) the vicinity of Gangneung city (third domain), respectively. A small circle in (a,b), an arrow, and a large black circle denote Gangneung city, airflow, and the vicinity of Gangneung city of inland and coastal sea, respectively. The dusts from Nei-Mongol into the city by the northwesterly wind in (a) combined with pollutants emitted from the city and then were trapped by the easterly wind in (b).

4.2.2. Effects of Wind and Atmospheric Boundary Layer on High PM Concentrations

Abrupt much higher PM₁₀ concentration of 180.78 $\mu\text{g}/\text{m}^3$ much larger than one before the dust period was detected at 09:00 LST, March 30 (the beginning time of office hour) (Figure 2). It must be attributed to that huge amounts of dust transported from both the Gobi Desert and Nei-Mongol along the eastern slope of Mt. Taegulyang toward the Gangneung coastal basin by the north-westerly wind could combine with particulate matter and gaseous emitted from vehicles on the road with its high density of the city, as usual (Figure 13a).

In the vicinity of the city in Figure 13b, the combined dust was further prohibited to move eastward by the westward onshore wind from the sea and trapped inside a smaller calm cavity generated by the confrontation of internal gravity waves in the lee side of the mountain under strong downslope wind (Figure 14a) than 09:00 LST, March 29, causing very high PM concentrations in Figure 2. After sunrise (here, at 09:00 LST), the thermal internal boundary layer due to the thermal heating of the ground surface starts to develop from the Gangneung coast toward the top of the Mt. Taegulyang along its eastern slope with about 200 m depth (Figure 14b). Thus, the combined dust should be trapped inside a shallow thermal internal boundary layer and were accumulated inside a calm cavity in Figure 14, showing very high ground-based PM concentration.

On mid-day, especially around 15:00 LST, March 30, PM₁₀ concentration was more or less than 50 $\mu\text{g}/\text{m}^3$, which was much larger than one before the dust period, but its magnitude is very small. Under northwesterly wind, huge amounts of dust were continuously transported from the Gobi Desert to Gangneung city, and had still combined with the local particulate matter and gaseous emitted from the vehicles on the road of the city.

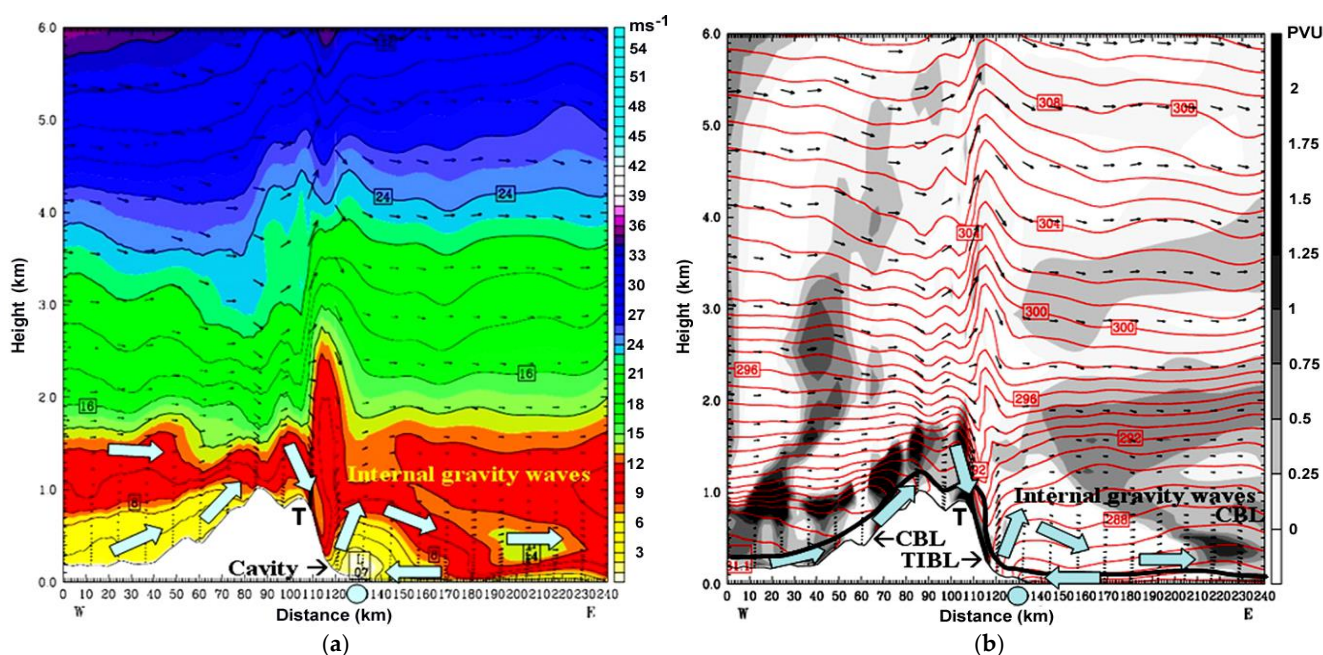


Figure 14. Vertical profile of (a) horizontal wind (m/s) and (b) potential temperature (K) and wind speed (m/s) simulated by WRF model at (a) 09:00 LST, 30 March 2004. Tick line, CBL, TIBL, T, and a small circle on the bottom of the figures denote the top of convective boundary layer, convective boundary layer, thermal internal boundary layer and Gangneung city, respectively. The dust transporting from the Nei-Mongo toward the Korean east coast moved down along the eastern slope of the mountain inside the TIBL and combined with pollutants emitted from the city. They were trapped inside a small calm cavity in (a) by the confront of IGW and easterly wind.

The combined pollutants were uplifted to the top of the TIBL due to the sufficient thermal convection of air near the ground surface and followed the propagation of eastward internal gravity waves to the East Sea without a calm cavity to be able to trap dust particles, resulting in very low PM concentrations near the surface of the city, as shown in Figure 15a,b, and Figure 2. However, the concentration of particulate matter is still much higher than that on March 29 before the dust period, due to the continuously supplied huge amounts of yellow dust from the Gobi Desert.

At the same time, the depth of CBL in the mountain basin in Figure 15b is about 1.2 km during the dust period, but compared to the depth of TIBL before the dust period, its depth in the coast is much shallower with about 100 m by weak thermal convection near the surface through the continuous accumulation of dust transported from the Gobi Desert toward the city. Its decreasing depth could cause an increasing dust density to have a much higher PM₁₀ concentration than one before the dust period at 15:00 LST.

At 20:00 LST, March 30, in the evening two hours after sunset, when huge amounts of dust from Nei-Mongo under northwesterly wind passed over Gangneung city in the Korean east coast, abrupt ground-based maximum concentrations of PM₁₀, PM_{2.5}, and PM₁ reached 238.87 µg/m³, 46.50 µg/m³ and 30.25 µg/m³ much higher than ones before the dust period, respectively (Figure 2).

In Figure 16a,b and Figure 17a,b, the northwesterly wind near Mt. Taegulyang in the west of Gangneung city was strong larger than 10 ms⁻¹. This strong wind accompanying huge amounts of dust from Nei-Mongo moved down along the eastern slope of the mountain and could be intensified into a strong downslope wind, which could generate internal gravity waves bounding up and down and propagating eastward.

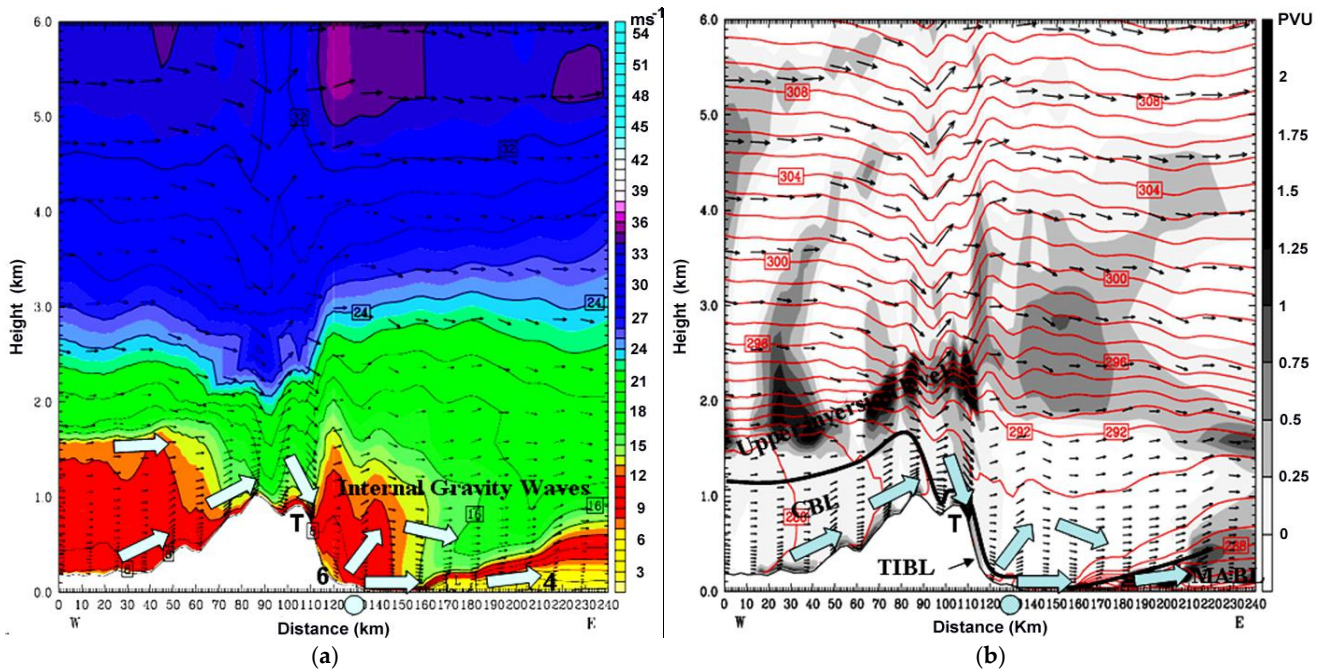


Figure 15. Vertical profile of (a) horizontal wind (m/s) and (b) potential temperature (k) and wind speed (m/s) in the third domain of WRF model simulation at (a) 15:00 LST, 30 March 2004. Tick line, CBL, TIBL, T, MABL and a small circle on the bottom of the figures denote the top of the convective boundary layer, convective boundary layer, thermal internal boundary layer, Mt. Taegulyang, marine atmospheric boundary layer, and Gangneung city, respectively.

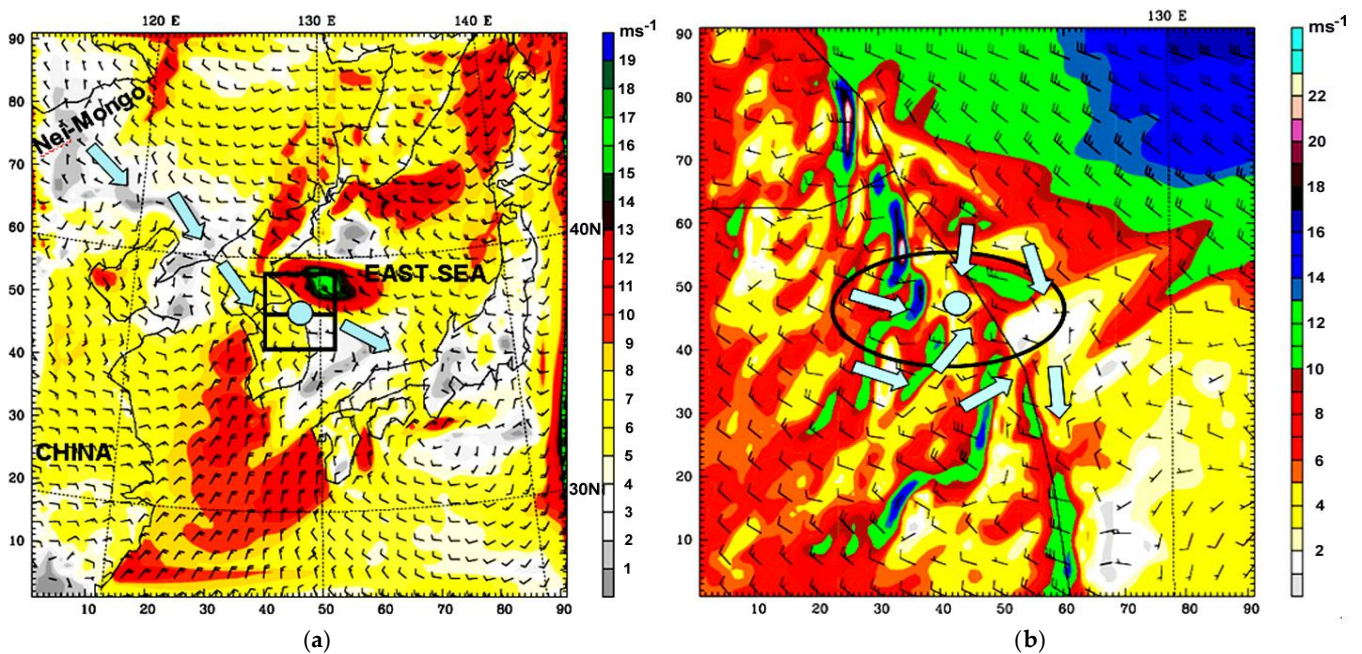


Figure 16. Surface wind (m/s) (a) in north-eastern Asia including Gangneung city on the Korean east coast (a small square) at 20:00 LST, 30 March 2004, and (b) the vicinity of Gangneung city, respectively. Arrow, a small circle in (a) and large and small circles in (b) denote air flow, Gangneung city, Gangneung city including its coast and downtown, respectively. Northwestern wind induced high amounts of dust from Nei-Mongo into Gangneung city in (a), and the transported dust combining with pollutants emitted from the city was trapped inside of the city by opposite easterly wind from the East Sea in (b), resulting in the maximum PM concentration.

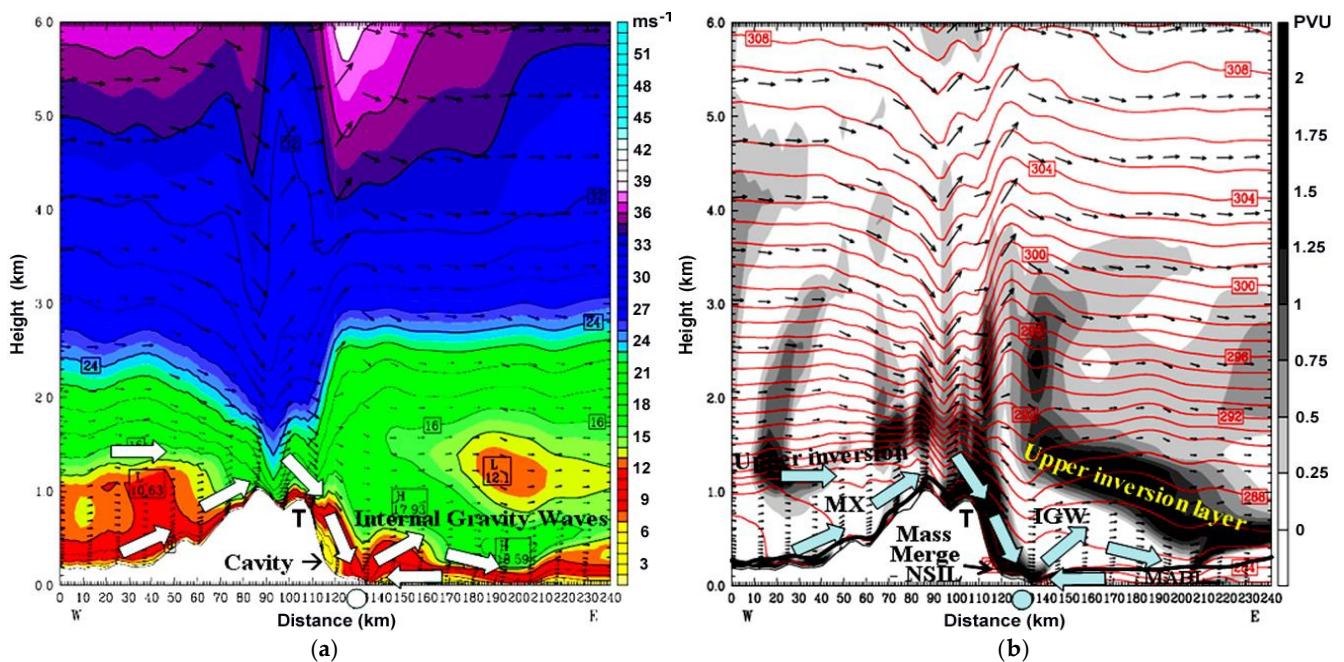


Figure 17. Vertical profile of (a) horizontal wind (m/s) and (b) potential temperature (k) and wind speed (m/s) in the third domain of WRF model at (a) 20:00 LST, 30 March 2004. NSIL, Tick line, MX, T, IGW and MABL and a small circle denote nocturnal surface inversion layer, its top, mixed layer, Mt. Taegulyang, internal gravity waves, marine atmospheric boundary layer and Gangneung city.

The transported dust should be merged inside a very shallow calm cavity (yellow color area near the coastal surface) generated by both westerly internal gravity waves and northeasterly wind from the sea toward the inland basin. At the same time, as the transported dust from China could combine again with particulate matter and gaseous emitted from not only many vehicles on the road for two hours after sunset (after the end of office hours), around 20:00 LST, March 30, but also nighttime heating boilers in the residential area of the city due to cold weather, all combined dust should be merged in the coast and caused high ground-based PM concentrations in the city.

At the same time, as nighttime cooling of the ground can cause the cooling of air masses near the ground surface, which can produce a stable and shallow nocturnal surface inversion layer (NSIL) (Figure 17b). The NSIL is much shrunken than the daytime CBL or the TIBL, and the stable atmospheric condition can suppress the uplifting of pollutants emitted from the city and induce the falling of floating particles during the day toward the ground surface, resulting in abrupt maximum PM concentrations at 20:00 LST, March 30, as shown in Figure 2.

5. Conclusions

The research to investigate the abrupt high PM concentrations gave the following results.

1. For a non-dust period before the influence of dust transported from the Gobi Desert and Nei-Mongo in northern China to a Korean east coastal city until 07:00 LST, March 29, PM_{10} , $\text{PM}_{2.5}$, and PM_1 concentrations at the city were very low and their maximum (minimum) values of each particulate matter (PM) concentrations were $72.33 \mu\text{g}/\text{m}^3$ ($12.53 \mu\text{g}/\text{m}^3$), $41.00 \mu\text{g}/\text{m}^3$ ($6.75 \mu\text{g}/\text{m}^3$), $35.33 \mu\text{g}/\text{m}^3$ ($5.82 \mu\text{g}/\text{m}^3$), respectively.

2. During the dust period from 08:00 LST, March 30~00:00 LST, April 2. under the intensive intrusion of yellow dust from the Gobi Desert toward the city by northwesterly wind, huge amounts of dust from Nei-Mongo in China passed over Gangneung city on the Korean east coast, PM_{10} , $\text{PM}_{2.5}$, and PM_1 concentrations in the city at 20:00 LST, March 30 reached $238.87 \mu\text{g}/\text{m}^3$, $46.50 \mu\text{g}/\text{m}^3$ and $30.25 \mu\text{g}/\text{m}^3$, and their minima were $41.68 \mu\text{g}/\text{m}^3$,

7.17 $\mu\text{g}/\text{m}^3$, and 2.77 $\mu\text{g}/\text{m}^3$, indicating their maxima being at least five times larger than their minima. Especially, maximum PM_{10} ($\text{PM}_{2.5}$ and PM_1) concentration for the dust period was 3.3 (1.1 and 1.01) times higher than one of the non-dust periods.

3. High PM_{10} ($\text{PM}_{2.5}$ and PM_1) concentrations were detected at 09:00 LST (just at the beginning time of office hours), as the transported dust transported could combine with particulates emitted from many vehicles in the city, and the combined dust was trapped inside a calm cavity generated by internal gravity waves in the lee side of the mountain and coast. Then, the eastward movement of the trapped dust was prohibited by easterly wind from the East Sea toward the mountain, resulting in the dust to be merged into the ground surface of the city, causing high PM concentrations at this time.

4. Around 15:00 LST, the thermal internal boundary layer developed up to 300 m in height from Gangneung city at the coast to the top of the mountain in its west along its slope. The combined dust from the Gobi Desert and both locally emitted particulate matter and gaseous from the vehicles on the road should be uplifted to the top of the thermal internal boundary layer (TIBL) due to the strong thermal convection from the ground surface, resulting in very low PM concentrations near the ground surface, but very high PM concentrations near the top of the TIBL.

5. After sunset, nocturnal cooling of the ground surface produces a stable nocturnal surface inversion layer (NSIL). This stable thermal condition could induce the falling of air pollutants which floated to the top of the TIBL for daytime hours and suppress the uplifting of air pollutants emitted for the nighttime hours, resulting in the pollutants to being merged near the ground surface. Thus, the combined huge amounts of dust transported from China with local particulates emitted from the city and dust of falling from the top of the stable inversion layer were trapped and accumulated in a calm cavity generated by internal gravity and easterly wind. Much shallower NSIL than the daytime TIBL could compress those accumulated pollutants and cause a great increase in pollutant concentration, like PM, showing the maximum PM concentrations at 20:00 LST.

Author Contributions: Conceptualization, D.-S.C. and H.C.; methodology, H.C., D.-S.C. and S.-M.C.; software, D.-S.C. and S.-M.C.; validation, H.C., D.-S.C. and S.-M.C.; formal analysis, H.C., D.-S.C. and S.-M.C.; investigation, D.-S.C. and S.-M.C.; resources, H.C., D.-S.C. and S.-M.C.; data curation, D.-S.C. and S.-M.C.; writing—original draft preparation, D.-S.C. and H.C.; writing—review and editing, H.C. and D.-S.C.; visualization, D.-S.C., H.C. and S.-M.C.; supervision, H.C.; project administration, H.C.; funding acquisition, H.C. All authors have read and agreed to the published version of the manuscript.

Funding: This research received no external funding.

Data Availability Statement: Hourly PM_{10} , $\text{PM}_{2.5}$ and PM_1 data at Gangneung city, Korea can be obtained from the data measured by H. Choi, D.-S. Choi and S.-M. Choi personally using GRIMM Model-1107, as Gangneung city did not established any measuring equipment of PM inside the city at that time. Satellite images were obtained from Korea Meteorological Administration (KMA), and these images are not released from the KMA any more, in present. The figures using HYSPLIT backward trajectory of air can be obtained by anyone to operate “Compute archive trajectories” of “HYSPLIT Trajectories” supported by NOAA Air Resources Laboratory. (<https://www.ready.noaa.gov/hypub-bin/trajtype.pl?runtype=archive> accessed on 22 December 2020).

Acknowledgments: The authors (D.-S. Choi, S.-M. Choi and H. Choi) express much thanks to the KMA for obtaining GOES-9 DCD satellite images and weather maps.

Conflicts of Interest: The authors declare no conflict of interest.

References

1. Chon, H. Historical records of yellow sand observations in China. *Res. Environ. Sci.* **1994**, *7*, 1–11.
2. Qian, Z.; Hu, Y. *Survey and Analysis for “93.5.5.” Strong Duststorm, Duststorm Research in China*; Meteorological Press: Beijing, China, 1997; pp. 37–43.
3. Wang, X.; Ma, Y.; Chen, H.; Wen, G.; Chen, S.; Tao, Z.; Chung, Y. The relation between sandstorms and strong winds in Xinjiang, China. *Water, Air, Soil Poll.: Focus* **2003**, *3*, 67–79. [[CrossRef](#)]

4. Choi, H.; Zhang, Y.H. Predicting duststorm evolution with vorticity theory. *Atmos. Res.* **2008**, *89*, 338–350. [[CrossRef](#)]
5. Chung, Y.S.; Yoon, M.B. On the occurrence of yellow sand and atmospheric loadings. *Atmos. Environ.* **1996**, *30*, 2387–2397. [[CrossRef](#)]
6. Kai, K.; Okada, Y.; Uchino, O.; Tabata, I.; Nakamura, H.; Takasugi, T.; Nikaido, Y. K.; Okada, Y.; Uchino, O.; Tabata, I.; Nakamura, H.; Takasugi, T.; Nikaido, Y. Lidar observation and numerical simulation of a Kosa (Asian dust) over Tsukuba, Japan during the spring of 1986. *J. Meteor. Soc. Japan* **1988**, *66*, 457–471. [[CrossRef](#)]
7. Natsagdorj, L.; Jugder, D. Statistics method for prediction of dust storms over the Gobi and steppe area in Mongolia in spring. In *Scientific Report*; Institute of Meteorology, Hydrology and Environment: Ulaanbaatar, Mongolia, 1992; pp. 1–83.
8. Chung, Y.S.; Kim, H.S.; Natsagdorj, L.; Jugder, D.; Chen, S.J. On yellow sand occurred during 1997–2000. *J. Korean Meteor. Soc.* **2001**, *37*, 305–316.
9. Duce, R.A.; Unni, C.K.; Ray, B.J.; Prospero, J.M.; Merrill, J.T. Long-range transport of soil dust from Asia to the tropical North Pacific: Temporal variability. *Science* **1980**, *209*, 1522–1524. [[CrossRef](#)]
10. Zhang, X.; Arimoto, R. Atmospheric trace elements over source regions for Chinese dust: Concentrations, sources and atmospheric deposition on the losses plateau. *Atmos. Environ.* **1993**, *27A*, 2051–2067. [[CrossRef](#)]
11. Zhang, Y.; Zhong, Y. The simulation and diagnosis for a strong wind associated with northeast low. *Acta Meteor. Sinica* **1985**, *43*, 97–105.
12. Tegen, I.; Fung, I. Modeling of mineral dust in the atmosphere: Source transport and optical thickness. *J. Geophys. Res.* **1994**, *99*, 22914–22987. [[CrossRef](#)]
13. Carmichael, G.R.; Hong, M.S.; Ueda, H.; Chen, L.L.; Murano, K.; Park, J.K.; Lee, H.; Kim, Y.; Kang, C.; Shim, S. Aerosol composition at Cheju Island, Korea. *J. Geophys. Res.* **1997**, *102*, 6047–6061. [[CrossRef](#)]
14. Choi, S.W.; Song, H.D. Variation of concentration of heavy metal during Yellow sand period of winter season at Taegu area. *Bull. Environ. Sci.* **1999**, *4*, 1–13.
15. Duan, J.; Chen, S.J.; Chung, Y.S. The numerical experiments of aerosol radiative effects. *Univ. Pekinensis.* **2000**, *36*, 95–101.
16. David, M.T.; Robert, J.F.; Douglas, L.W. April 1998 Asian dust event: A southern California perspective. *J. Geophys. Res.* **2001**, *106*, 18371–18379. [[CrossRef](#)]
17. Gao, Y.; Anderson, J.R. Characteristics of Chinese aerosols determined by individual particle analysis. *J. Geophys. Res.* **2001**, *106*, 18037–18045. [[CrossRef](#)]
18. Kim, K.W.; Kim, Y.J.; Oh, S.J. Visibility impairment during Yellow Sand periods in the urban atmosphere of Kwangju, Korea. *Atmos. Environ.* **2001**, *35*, 5157–5167. [[CrossRef](#)]
19. Lin, T.H. Long-range transport of yellow sand to Taiwan in spring 2000: Observed evidence and simulation. *Atmos. Environ.* **2001**, *35*, 5873–5882. [[CrossRef](#)]
20. McKendry, I.G.; Hacker, J.P.; Stull, R.; Sakiyama, S.; Mignacca, D.; Reid, K. Long-range transport of Asian dust to the lower Fraser Valley, British Columbia, Canada. *J. Geophys. Res.* **2001**, *106*, 18361–18370. [[CrossRef](#)]
21. Kim, H.K.; Kim, M.Y.; Kim, J.; Lee, G. The concentrations and fluxes of total gaseous mercury in a western coastal area of Korea during the late March period of 2001. *Atmos. Environ.* **2002**, *36*, 3413–3427. [[CrossRef](#)]
22. Chung, Y.S.; Kim, H.S.; Jugder, D.; Natsagdorj, L.; Chen, S.J. On sand and duststorms and associated significant dustfall observed in Chongju-Chongwon, Korea. *Water, Air, Soil Pol. Focuss* **2003**, *3*, 5–19. [[CrossRef](#)]
23. Kim, H.K.; Kim, M.Y. The effects of Asian dust on particulate matter fractionation in Seoul, Korea during spring 2001. *Atmos. Environ.* **2003**, *51*, 707–721. [[CrossRef](#)] [[PubMed](#)]
24. Choi, H.; Choi, D.S. Concentrations of PM₁₀, PM_{2.5}, and PM₁ influenced by atmospheric boundary layer in the Korean mountainous coast during a duststorm. *Atmos. Res.* **2008**, *89*, 330–337. [[CrossRef](#)]
25. Choi, H.; Zhang, Y.H.; Kim, K.H. Sudden high concentration of TSP affected by atmospheric boundary layer in Seoul metropolitan area during duststorm period. *Environ. Internat.* **2008**, *34*, 635–647. [[CrossRef](#)]
26. Choi, H.; Zhang, Y.H.; Takahashi, S. Recycling of suspended particulates by the interaction of sea-land breeze circulation and complex coastal terrain. *Meteor Atmos. Phys.* **2004**, *87*, 109–120. [[CrossRef](#)]
27. Choi, H.; Speer, M.S. Effects of atmospheric circulation and boundary layer structure on the dispersion of suspended particulates in the Seoul metropolitan area. *Meteor. Atmos. Phys.* **2005**, *92*, 239–254. [[CrossRef](#)]
28. Holton, J.R. *An Introduction to Dynamic Meteorology*, 3rd ed.; Academic Press: New York, NY, USA, 1992; pp. 198–203.
29. Choi, H. Cold sea waters induced by cyclogenesis in the East Sea. *Dis. Advan.* **2013**, *6*, 12–20.
30. Choi, D.S. The Effects of Meteorological Conditions and Dusts Transported from Gobi Desert on Hourly Variations of Particulate Matter Concentrations (PM₁₀, PM_{2.5} and PM₁) and Their Regressive Predictions at Gangneung during a Yellow Sand Period in Spring. Master's Thesis, Chungnam National University, Chengju, Republic of Korea, 2013; pp. 1–88.
31. Rossby, C.G. Isentropic analysis. *Bull. Am. Meteor. Soc.* **1937**, *18*, 201–209. [[CrossRef](#)]
32. Rossby, C.G. Planetary flow patterns in the atmosphere. *Q. J. R. Meteorol. Soc.* **1940**, *66*, 68–87.
33. Reed, R.J.; Sanders, F. An investigation of the development of a mid-tropospheric frontal zone and its associated vorticity field. *J. Atmos. Sci.* **1953**, *10*, 338–349. [[CrossRef](#)]
34. Sanders, F.; Gyakum, J.R. Synoptic-dynamic climatology of the bomb. *Mon. Wea. Rev.* **1980**, *108*, 1589–1606. [[CrossRef](#)]
35. Reed, R.J.; Albright, M.D. A case study of explosive cyclogenesis in the Eastern Pacific. *Mon. Wea. Res.* **1986**, *114*, 2297–2319. [[CrossRef](#)]

36. Chen, S.J.; Kuo, Y.H.; Zhang, Y.H. Synoptic climatology of cyclogenesis over east Asia, 1958–1987. *Mon. Wea. Rev.* **1991**, *119*, 1407–1418. [[CrossRef](#)]
37. Haynes, P.H.; McIntyre, M.E. On the evolution of vorticity and potential vorticity in the presence of diabatic heating and frictional or other forces. *J. Atmos. Sci.* **1987**, *44*, 828–841. [[CrossRef](#)]
38. Choi, H.; Choi, D.S.; Choi, S.-M. Meteorological condition and atmospheric boundary layer influenced upon temporal concentrations of PM₁, PM_{2.5} at a coastal city, Korea for Yellow Sand event. *Dis. Advan.* **2010**, *3*, 309–315.

Disclaimer/Publisher’s Note: The statements, opinions and data contained in all publications are solely those of the individual author(s) and contributor(s) and not of MDPI and/or the editor(s). MDPI and/or the editor(s) disclaim responsibility for any injury to people or property resulting from any ideas, methods, instructions or products referred to in the content.